

2,3-dichloropropionic acid, 565-64-0; 2,3-dichloropropionyl chloride, 7623-13-4.

References and Notes

- (1) British Patent, 411 860; *Chem. Abstr.* **1934**, 28, 6956.
- (2) Marvel, C. S.; Cowan, J. C. *J. Am. Chem. Soc.* **1939**, 61, 3156.
- (3) Marvel, C. S.; Dec, J., Cooke, H. G., Jr.; Cowan, J. C. *J. Am. Chem. Soc.* **1940**, 62, 3495.
- (4) Dever, G. R.; Karasz, F. E.; MacKnight, W. J.; Lenz, R. W. *J. Polym. Sci., Polym. Chem. Ed.* **1975**, 13, 2151.
- (5) Dever, G. R.; Karasz, F. E.; MacKnight, W. J.; Lenz, R. W. *J. Polym. Sci., Polym. Chem. Ed.* **1975**, 13, 1803.
- (6) Helbert, J. N.; Poindexter, E. H.; Pittman, C. U., Jr.; Chen, C. Y. *Polym. Eng. Sci.* **1980**, 20, 630.
- (7) Lai, J. H.; Shrawagi, S. *J. Appl. Polym. Sci.* **1978**, 22, 53.
- (8) Lai, J. H.; Helbert, J. N.; Cook, C. F., Jr.; Pittman, C. U., Jr. *J. Vac. Sci. Technol.* **1979**, 16, 1992.
- (9) Chen, C. Y.; Mohammad, I.; Pittman, C. U. Jr.; Helbert, J. N. *Makromol. Chem.* **1978**, 179, 2109.
- (10) Helbert, J. N.; Caplan, P. J.; Poindexter, E. H. *J. Appl. Polym. Sci.* **1977**, 21, 797.
- (11) Babu, G. N.; Lu, P. H.; Hsu, S. L.; Chien, J. C. W. *J. Polym. Sci., Polym. Chem. Ed.* **1984**, 22, 195.
- (12) Perrin, D. D.; Armarego, W. L. F.; Perrin, D. R. "Purification of Laboratory Chemicals"; 2nd ed.; Pergamon Press: Oxford, 1980.
- (13) Riddick, J. A.; Bunge, U. B. "Organic Solvents"; Wiley: New York, 1970.
- (14) Dyer, J. R. "Application of Absorption Spectroscopy of Organic Compounds"; Prentice Hall: Delhi, 1971.
- (15) Patnak, C. P.; Patini, M. C.; Babu, G. N.; Chien, J. C. W. *Makromol. Chem.*, in press.
- (16) Dhal, P. K.; Nanada, S.; Babu, G. N. *Macromolecules* **1984**, 17, 1131.
- (17) Schaefer, J.; Natusch, D. F. S. *Macromolecules* **1972**, 5, 416.
- (18) Wehrli, F. W.; Wirtlin, T. "Interpretation of Carbon-13 NMR Spectra"; Hyden: 1976, p 264.
- (19) Heatley, F.; Begum, A. *Polymer* **1976**, 17, 399.
- (20) Randall, J. C. *J. Polym. Sci., Polym. Phys. Ed.* **1976**, 14, 1693.
- (21) Hatada, K.; Kitayama, T.; Okamoto, Y.; Ohta, K.; Umemura, Y.; Yuki, H. *Makromol. Chem.* **1977**, 178, 617.
- (22) Lyeria, J. R., Jr.; Horikawa, T. T.; Johnson, D. E. *J. Am. Chem. Soc.* **1977**, 99, 2463.
- (23) Hatada, K.; Kitayama, T.; Lenz, R. W. *Makromol. Chem.* **1978**, 179, 1951.
- (24) Hatada, K.; Kitayama, T.; Saunders, K.; Lenz, R. W. *Makromol. Chem.* **1981**, 182, 1449.
- (25) Watanabe, H.; Murano, M. *J. Polym. Sci. Part A-1* **1971**, 9, 911.
- (26) Bovey, F. A. "Chain Structure and Conformation of Macromolecules"; Academic Press: New York, 1982.
- (27) Yuki, H.; Okamoto, Y.; Shimada, Y.; Ohta, K.; Hatada, K. *Polymer* **1976**, 17, 618.
- (28) Yuki, H.; Hatada, K.; Niimomi, T.; Kikuchi, Y. *Polym. J. (Tokyo)* **1970**, 1, 36.
- (29) Bovey, F. A. "High Resolution NMR of Macromolecules"; Academic Press: New York, 1972.

Magnetic Properties of Very Low and Very High Molecular Weight Polyacetylenes

James C. W. Chien* and Michael A. Schen†

Department of Chemistry and Department of Polymer Science and Engineering, Materials Research Laboratory, University of Massachusetts, Amherst, Massachusetts 01003.
Received September 6, 1985

ABSTRACT: Magnetic properties of $[\text{CH}]_x$ with number-average molecular weight (\bar{M}_n) from 480 to 870 000 have been studied and compared with those with $\bar{M}_n \sim 11\,000$ prepared by the standard Ito-Shirakawa-Ikeda procedure. The very low \bar{M}_n *cis*- $[\text{CH}]_x$ has a T_1 value of ca. 190 μs , which decreases with increasing molecular weight (MW). The values of T_1 of *trans*- $[\text{CH}]_x$ are also MW dependent, decreasing from $64 \pm 22\ \mu\text{s}$ to about 20 μs , but T_2 increases from $64 \pm 22\ \text{ns}$ to ca. 100 ns with increasing MW. The unpaired-spin concentrations $[\text{S}\cdot]$ for *cis*- $[\text{CH}]_x$ are quite variable from sample to sample for all MW. Upon heating, *cis*- $[\text{CH}]_x$ isomerizes to *trans*- $[\text{CH}]_x$ with a relatively constant $[\text{S}\cdot]_m$ of $(4.8 \pm 1.2) \times 10^{-4}$ spins/CH for all polymers. Iodine doping of *trans*- $[\text{CH}]_x$ has no effect on $[\text{S}\cdot]_m$ until $y(\text{I}_3^-) \sim 3 \times 10^{-4}$, above which $[\text{S}\cdot]$ decreases rapidly with increasing doping. In the case of *cis*- $[\text{CH}]_x$ light doping increases $[\text{S}\cdot]$, but the trend is reversed above $y \sim 3 \times 10^{-4}$. Iodine doping of *trans*- $[\text{CH}]_x$ decreases T_1 monotonically beginning at the ppm level of I_3^- , whereas T_2 remains constant until $y = (1-3) \times 10^{-4}$ before its value decreases. In contrast, for $0 < y < 1.7 \times 10^{-3}$, iodine-doped low MW *cis*- $[\text{CH}]_x$ has constant values of $T_1 = 187 \pm 54\ \mu\text{s}$, $T_2 = 11.6 \pm 0.8\ \text{ns}$, and $\Delta H_{pp} = 5.6 \pm 0.4\ \text{G}$. The EPR cannot be saturated at higher dopant concentration. When EPR is observable, it has a Lorentzian line shape and a Curie temperature dependence. The above effects of doping are the same for polymers of different MW. These results are interpreted to mean interchain spin diffusion or hopping is the determinant for some aspects of spin dynamics.

Introduction

Polyacetylene can be synthesized with predominantly *cis* or *trans* structures.¹ The former can be thermally isomerized to the latter, which is the thermodynamically stable form.² Most *trans*- $[\text{CH}]_x$ specimens are prepared by this method instead of the alternate ones by high-temperature polymerization or doping or compensation. *trans*- $[\text{CH}]_x$ is said to be unstable toward a commensurate Peierls distortion (index of 2) to a bond-alternate semiconducting state.³ The neutral topological defect is said to have soliton wavelike characteristics.⁴ Many spectro-

scopic and transport properties have been interpreted as the manifestation of solitons.⁵ Solitons cannot exist in *cis*- $[\text{CH}]_x$ because the neutral defect is confined in this polymer. Differences in the EPR of the unpaired spins in the two isomers were the first evidence cited for the existence of solitons.⁶ The diffusion of a soliton should be one-dimensional. There have been various attempts to estimate the anisotropy through the analysis of EPR line shape, proton T_1 , dynamic nuclear polarization, and spin-echo data. We have used the effect of dopant on EPR saturation⁷ to obtain the diffusion coefficients in *trans*- $[\text{CH}]_x$: $D_{\parallel} = 3.8 \times 10^{14}\ \text{s}^{-1}$ and $D_{\perp} = 1.1 \times 10^9\ \text{s}^{-1}$. Therefore, there is a nonnegligible off-chain component to the spin dynamics, which can be further investigated by the EPR of $[\text{CH}]_x$ of different molecular weights (MW).

* To whom inquiries should be addressed.

† Present address: Polymeric Materials Division, National Bureau of Standards, Gaithersburg, MD.

Polyacetylene is insoluble and infusible, so that its MW cannot be determined by conventional methods. However, the number-average molecular weight (\bar{M}_n) can be obtained by tagging each chain with tritium followed by radioassay.⁸ A detailed study of the kinetics of acetylene polymerization⁹ gave the effects of catalyst ratio, concentration, aging, monomer pressure, temperature, and polymerization time on the yields and \bar{M}_n of $[\text{CH}]_x$. From these results it was possible to select polymerization conditions to produce $[\text{CH}]_x$ with \bar{M}_n ranging from 400 to 870 000.¹⁰

In this paper we present results of a detailed study of the EPR of both undoped and doped *cis*- and *trans*- $[\text{CH}]_x$ of polymers with $\bar{M}_n = 500$ (L- $[\text{CH}]_x$), and high MW polymers (H- $[\text{CH}]_x$ -(N), where the number N in parentheses is $\bar{M}_n \times 10^{-4}$). The results are compared to those of standard polymers (S- $[\text{CH}]_x$), prepared by the Shirakawa procedure¹ which have $\bar{M}_n \sim 11\,000$.⁸

Experimental Techniques

Samples. S- $[\text{CH}]_x$ films were prepared by a procedure^{8b} adapted from that of Ito et al.¹ *cis*- $[\text{CH}]_x$ with \bar{M}_n from 400 to 920 000 were synthesized with methods given elsewhere.¹⁰ To reduce the Ti and Al residues, the polymer films were washed more than 12 times with freshly distilled toluene or pentane, treated with dry, oxygen-free 10% HCl-methanol, and further washed 3 times with methanol. After the specimens were vacuum-dried, they were stored in a Schlenk vessel under an argon atmosphere at 195 K and used for measurement within a week of preparation.

Slow and homogeneous doping of $[\text{CH}]_x$ with iodine was performed as previously described.^{7,11} For low dopant levels of $y < 10^{-3}$, where y is moles of I_3^- dopant per CH, $^{125}\text{I}_2$ was used and its concentration obtained by radioassay.

EPR. A Varian E-9 X-band spectrometer was used in the EPR studies. Saturation measurements and calculations of T_1 and T_2 have been described.⁷ Spin concentrations were obtained by double integration of the EPR spectra and compared with a tetramethylpiperidinoxyl standard at the same microwave frequency and detector current.¹¹

Results

Undoped *cis*- $[\text{CH}]_x$. Acetylene polymerized in an EPR sample tube at 195 K has apparently defect-free *cis*-transoid structure because there is no observable $g = 2$ signal.¹² A weak, broad, EPR signal develops upon warming the polymer to room temperature and is attributable to thermal *cis*-trans isomerization. This isomerization is catalyzed by oxygen.¹³ We have measured the spin concentration $[\text{S}\cdot]$ in spins per CH unit for *cis*- $[\text{CH}]_x$ having a range of MW and for different preparations of the same \bar{M}_n . Four preparations of L-*cis*- $[\text{CH}]_x$ have $[\text{S}\cdot]$ values of 1.3×10^{-5} , 4.5×10^{-5} , 6.1×10^{-5} , and 7.9×10^{-5} spins/CH. The range of $[\text{S}\cdot]$ found in this work and previously¹³ for S-*cis*- $[\text{CH}]_x$ is $(2.0\text{--}4.0) \times 10^{-5}$ spins/CH. A sample of H-*cis*- $[\text{CH}]_x$ -(7.5), where (7.5) denotes $\bar{M}_n = 75\,000$ (vide supra), has $[\text{S}\cdot] = 1.3 \times 10^{-5}$ spins/CH. Therefore, there is significant variation of $[\text{S}\cdot]$ from one preparation to another of the same MW, which is most likely due to different thermal histories of the polymers and any exposure to air. There is also no trend of $[\text{S}\cdot]$ dependence on MW up to $\bar{M}_n = 7.5 \times 10^4$. However, there is no detectable EPR for very high MW samples of *cis*- $[\text{CH}]_x$ with \bar{M}_n between 2.5×10^5 and 8.7×10^5 . It is possible that the conditions of polymerization to high MW product lead to very pure *cis* structure. Also, we have found¹⁰ that the *cis*-trans isomerization is slower for high MW polymers than it is for low MW *cis*- $[\text{CH}]_x$ (vide infra).

A room-temperature EPR saturation curve had been obtained for L-*cis*- $[\text{CH}]_x$. There is only a slight increase of 14% in line width above saturation; the line width at low microwave power is 5.5 G. The values of T_1 and T_2

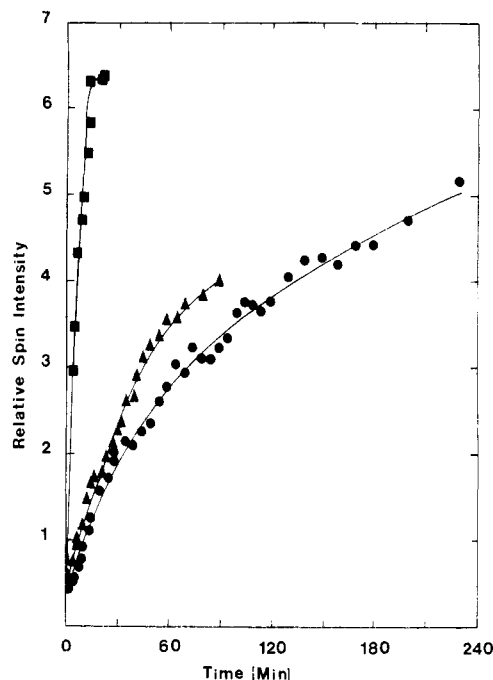


Figure 1. Increase in unpaired-spin concentration with isomerization time for L- $[\text{CH}]_x$ at (●) 383 K, (▲) 423 K, and (■) 453 K.

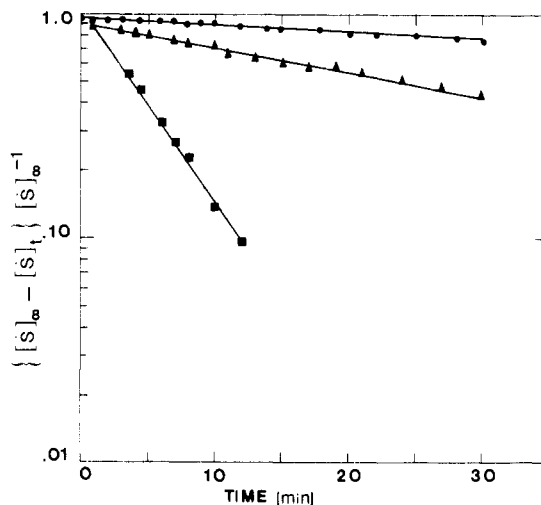


Figure 2. First-order kinetic plot of the data in Figure 1. The legends are the same.

are 190 μs and 12 ns, respectively. These are to be compared with $T_1 = 54 \pm 9 \mu\text{s}$ and $T_2 = 10 \pm 0.7 \text{ ns}$, respectively, for S-*cis*- $[\text{CH}]_x$.⁷ Therefore, the T_1 is much longer for the $\bar{M}_n = 500$ polymer than the $\bar{M}_n = 11\,000$ polymer.

Thermal Isomerization. When *cis*- $[\text{CH}]_x$ is heated, there is isomerization to the *trans* isomer² and creation of neutral defects.¹² The two processes are not simply related; for the S- $[\text{CH}]_x$ samples a linear plot was found for $\log [\text{S}\cdot]$ vs. *trans* content, where $[\text{S}\cdot]$ is the unpaired-spin concentration. L- $[\text{CH}]_x$ was found to isomerize with greater ease and more completely than S- $[\text{CH}]_x$ under similar conditions.¹⁰ In this work the increase of $[\text{S}\cdot]$ with time of heating of L- $[\text{CH}]_x$ was monitored at several temperatures (Figure 1). The process obeys first-order kinetics as shown in Figure 2; the rate constants are compared with those obtained for S- $[\text{CH}]_x$ in Table I. The unpaired spins are formed at a much slower rate for L- $[\text{CH}]_x$ than for S- $[\text{CH}]_x$, but the activation energies are about the same. The data in Figure 3 further attested to this MW dependence. The rate of decrease in EPR line width with time of

Table I
Kinetics of Formation of Unpaired Spins in $[\text{CH}]_x$

temp, K	first-order rate constant, s^{-1}	
	L- $[\text{CH}]_x$	S- $[\text{CH}]_x^{6c}$
348		2.7×10^{-4}
383	1.05×10^{-4}	
398		1.85×10^{-3}
423	2.72×10^{-4}	
453	1.22×10^{-3}	
activation energy, kcal mol $^{-1}$	12	12

Table II
Unpaired-Spin Concentrations in *trans*- $[\text{CH}]_x$

no.	\bar{M}_n	isomerization conditions		$[\text{S}] \times 10^4$ spins per CH
		temp, K	time, min	
1	400	453	20	6.25
2	400	453	20	5.9
3	500	383	1600	4.0
4	500	423	90	3.3
5	500	453	12	5.0
6	500	453	20	3.3
7	500	483	5	4.8
8	5300	453	15	3.45
9	5300	453	15	3.2
10	6200	453	15	4.3
11	10500	383	1440	5.56
12	10500	418	240	4.8
13	10500	441	120	5.56
14	10500	468	90	6.25
15	10500	417	30	7.7
16	25000	453	40	5.0
17	210000	453	20	4.8
18	210000	453	20	5.0
19	870000	423	90	3.7
20	870000	423	200	5.3

av 4.8 ± 1.2

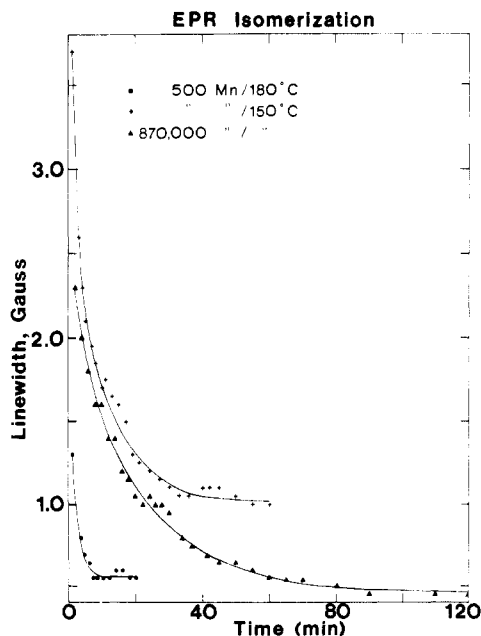


Figure 3. Decrease of EPR line width with time of isomerization for (●) L- $[\text{CH}]_x$ at 453 K, (+) L- $[\text{CH}]_x$ at 423 K, (▲) H- $[\text{CH}]_x$ (87) at 423 K.

heating at 423 K is more rapid, and the instantaneous and limiting line widths are narrower for the very high MW ($\bar{M}_n = 870\,000$) samples than for the very low MW ($\bar{M}_n = 500$) polymer. Increasing the temperature of isomerization to 453 K greatly increases the rate of narrowing of the EPR line width of L- $[\text{CH}]_x$ to a value of about 0.6 G.

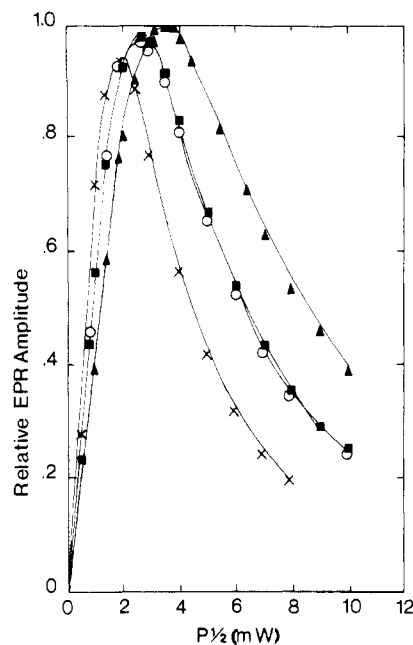


Figure 4. EPR saturation curves of *trans*- $[\text{CH}]_x$ of \bar{M}_n (x) 500, (■) 10 500, (▲) 210 000, and (○) 870 000.

Table III
EPR Relaxation Times for *trans*- $[\text{CH}]_x$

no. ^a	ΔH_{pp} , G	$T_1 \times 10^6$, s	$T_2 \times 10^9$, s
3	1.5	100	44
4	2.4	40	27
5	1.2	60	55
6	1.1	55	60
7	0.95	64	69
	av 1.4 ± 0.6	64 ± 22	51 ± 16
11	1.8	30	36
12	0.95	28	69
13	0.83	24	79
14	0.80	27	82
15	1.0	29	66
	av 1.1 ± 0.5	28 ± 5	66 ± 18
S- <i>trans</i> - $[\text{CH}]_x^b$		27 ± 2	78 ± 10
16	0.6	30	110
17	0.6	10	110
19	0.8	18	80
20	0.7	20	94

^a As in Table II. ^b Reference 7.

Undoped *trans*- $[\text{CH}]_x$. The unpaired-spin concentration of S- $[\text{CH}]_x$ is reported by various laboratories to have values of 3×10^{-4} to 10^{-3} spins per CH unit. Even more remarkable is that this $[\text{S}]$ is independent of MW and insensitive to isomerization conditions. It is shown in Table II that *trans*- $[\text{CH}]_x$ with \bar{M}_n from 400 to 870 000 isomerized from the *cis* polymers at temperatures ranging from 383 to 453 K for 5–1600 min have the same average $[\text{S}]_m = (4.6 \pm 0.9) \times 10^{-4}$ spins per CH unit.

Figure 4 illustrates typical EPR saturation curves for different MW *trans*- $[\text{CH}]_x$. The relaxation times are summarized in Table III. There appear to be some trends of decrease of T_1 and an increase of T_2 with increasing MW. The most pronounced difference is the T_1 values of L- and S-*trans*- $[\text{CH}]_x$ samples. Therefore, the longer T_1 for L-*cis*- $[\text{CH}]_x$ than higher MW *cis* polymers (vide supra) is also seen for *trans* isomers of different MW.

The EPR line width increases with increasing microwave power in excess of the power for maximum EPR amplitude (Figure 5): the effect is greater for the lower MW polymers.

Iodine-Doped *cis*- $[\text{CH}]_x$. Since undoped *cis*- $[\text{CH}]_x$ has very low and variable $[\text{S}]$, it is difficult to determine the

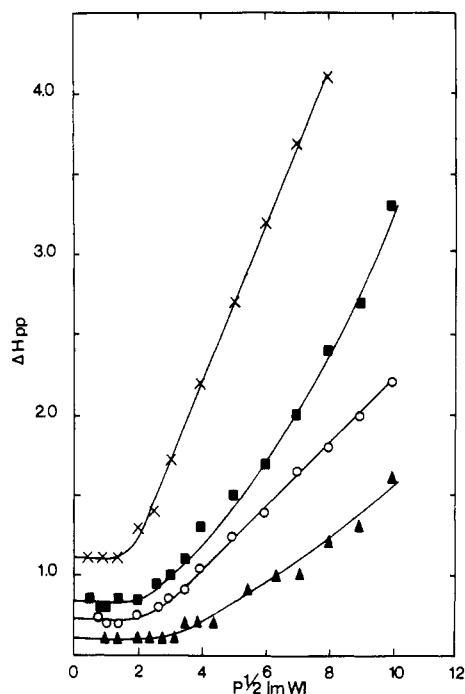


Figure 5. Variation of EPR line width with microwave power for *trans*-[CH]_x. Legends are the same as Figure 4.

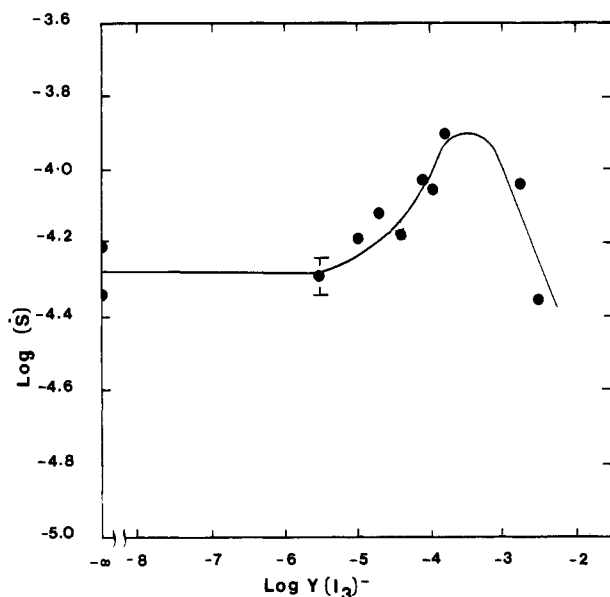


Figure 6. Effect of iodine doping on [S·] in *L-cis*-[CH]_x.

precise effect of doping on [S·]. In this work, there seems to be a consistent effect, as illustrated in Figure 6. For instance, [S·] for different *L-cis*-[CH]_x preparations that have initial undoped values of $(1.6\text{--}5.0) \times 10^{-5}$ spin/CH begins to increase when $\gamma(I_3^-)$ exceeds 10^{-5} and approaches a common maximum value of [S·] $\sim 10^{-4}$, observed at $\gamma(I_3^-) \sim 3 \times 10^{-4}$. The value of [S·] decreases rapidly with further doping. These results are in good agreement with previous measurements on S-[CH]_x⁷ where the EPR signal amplitude decreased as $\gamma(I_3^-) \geq 3 \times 10^{-4}$ (note that in ref 7 γ was given in moles of I/CH) and disappeared at a maximum doping level of ca. 5 mol % I_3^- . In the case of *L-cis*-[CH]_x, the maximum doping level is only 0.3 mol % I_3^- and a very weak EPR signal could still be detected.

All EPR spectra of iodine-doped *L-cis*-[CH]_x have Lorentzian line shape and nearly the same line width of 5.6 ± 0.4 G. The latter is insensitive to microwave power. The spin-lattice and spin-spin relaxation times are in-

Table IV
EPR and Relaxation Data for Iodine-Doped *L-cis*-[CH]_x

$\gamma(I_3^-)$	ΔH_{pp} , G ^a	T_1 , μ s	T_2 , ns
0	5.8	186	11
3.4×10^{-6}	6.4	143	10
1.15×10^{-5}	5.3	158	12
2×10^{-5}	5.3	170	12
4.3×10^{-5}	5.7	286	11.5
1.2×10^{-4}	5.3	177	12
2×10^{-4}	5.0	251	13
1.7×10^{-3}	5.7	127	11.5
	av 5.6 ± 0.4	187 ± 54	11.6 ± 0.8
3.2×10^{-3}	4.6	ns ^b	

^a EPR line width at low microwave power. ^b No saturation.

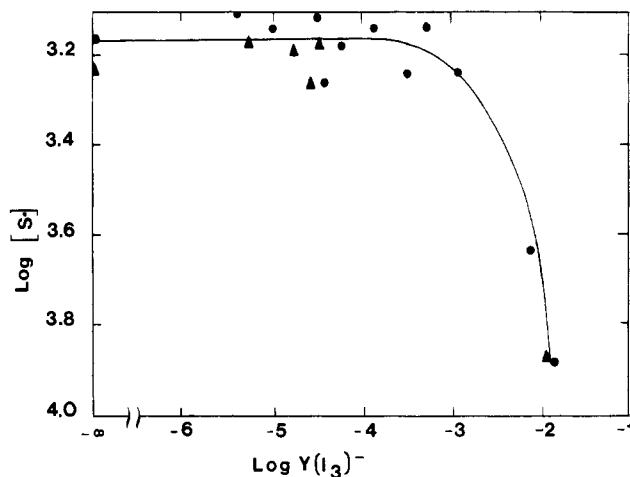


Figure 7. Variations of [S·] with γ for iodine-doped $\bar{M}_n = 500$ trans polymers: (●) [CH]_x; (▲) [CD]_x.

dependent of dopant concentration. However, the EPR cannot be saturated at the highest $\gamma(I_3^-) = 3.2 \times 10^{-3}$. At lower dopant concentrations, Table IV shows that $T_1 = 187 \pm 54$ μ s and $T_2 = 11.6 \pm 0.8$ ns. These behaviors are apparently independent of MW because they are the same for both *L-cis*-[CH]_x and *S-cis*-[CH]_x.⁷

The unpaired-spin concentration for *L-cis*-[CH(I₃)_y]_x increases 1.3-fold with the decrease of temperature from 293 to 133 K. The variation is the same for $3 \times 10^{-6} \leq \gamma \leq 10^{-3}$.

Iodine-Doped *trans*-[CH]_x. Undoped *trans*-[CH]_x and *trans*-[CD]_x have relatively constant values of [S·]_m (Table II). This [S·]_m is apparently unaffected by a low level of iodine doping up to about $\gamma = 3.3 \times 10^{-4}$ (Figure 7) for *L-trans*-[CH]_x as well as *L-trans*-[CD]_x. With higher iodine doping [S·] decreases rapidly with increasing γ . These behaviors are identical with those reported for S-[CH]_x⁷ and observed as well for very high MW H-*trans*-[CH]_x-(21) (Figure 8) on a limited number of measurements. For this polymer the decrease of [S·] appears to occur at slightly higher dopant level of ca. $10^{-3} I_3^-$, and the slope of the decrease for $\gamma > 10^{-3}$ is less steep than that of L-[CH]_x (compare Figures 7 and 8). Also the EPR signal disappeared at $\gamma = 0.12$ for H-*trans*-[CH(I₃)_y]_x-(21). It is recalled that¹⁴ Pauli susceptibility emerges in S-*trans*-[CH(I₃)_y]_x for $\gamma \geq 0.02$.

The T_1 for *L-trans*-[CH(I₃)_y]_x is decreased by ppm of dopant, for instance at $\gamma = 4.6 \times 10^{-6}$. The value of T_1 decreased monotonically with increasing γ , as shown in Figure 9. Similar effects were observed for the perdeuterated polymers (Figure 10 and Table V). The EPR cannot be saturated at $\gamma = 1.3 \times 10^{-2}$. The T_2 values for *L-trans*-[CH(I₃)_y]_x remained relatively constant at $(44 \pm 6) \times 10^{-9}$ s for $0 \leq \gamma \leq 1.3 \times 10^{-3}$. At higher doping concentrations of $\gamma = 8.4 \times 10^{-3} = 1.5 \times 10^{-2}$, the T_2 decreases

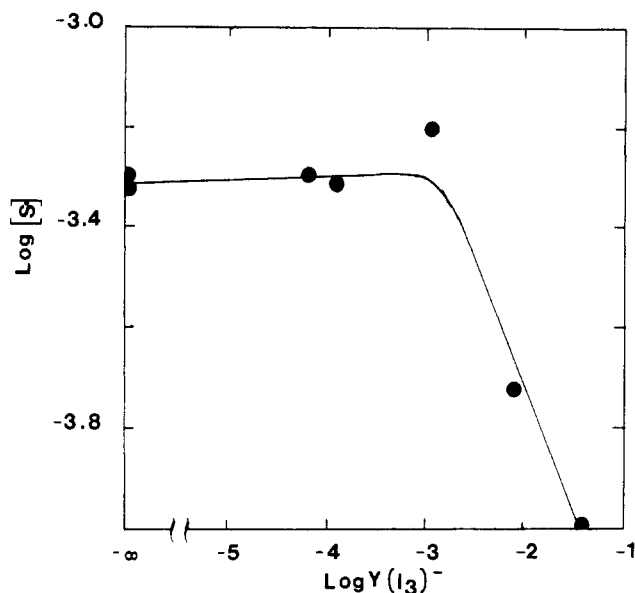


Figure 8. Variation of $[S]$ with y for iodine-doped $\bar{M}_n = 210\,000$ $trans\text{-}[CH]_x$.

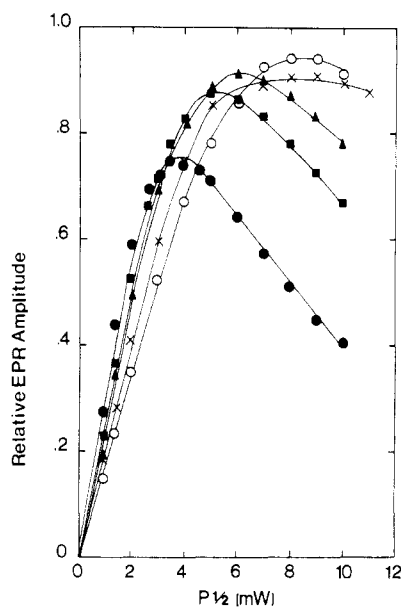


Figure 9. EPR saturation plots of $L\text{-}trans\text{-}[CH(I_3)_y]_x$ for y values (●) 0, (■) 3.4×10^{-5} , (▲) 3.5×10^{-4} , (+) 5.5×10^{-4} , and (○) 8.5×10^{-3} .

Table V
EPR Relaxation Times for $L\text{-}trans\text{-}[CD(I_3)_y]_x$

$y(I_3^-)$	ΔH_{pp} , G	$T_1 \times 10^6$, s	$T_2 \times 10^9$, s
0	0.5	39	130
5.5×10^{-6}	0.65	26	100
3.2×10^{-5}	0.60	24	110
7.4×10^{-3}	1.2	6	55
1.2×10^{-2}	2.1	ns ^a	31

^a Does not saturate.

significantly to 21 and 14 ns, respectively. Similar behaviors were observed for perdeuterated polymers (Table V).

The T_1 for $H\text{-}trans\text{-}[CH]_x$ (87) is about 3 times shorter than that of $L\text{-}trans\text{-}[CH]_x$ (Table III). We have limited data on the $\bar{M}_n = 870\,000$ polymer; however, Figure 11 shows an increase of microwave saturation power and thus a decrease of T_1 with light iodine doping. All the very high MW samples have nearly the same $T_2 = (80 \pm 7) \times 10^{-9}$

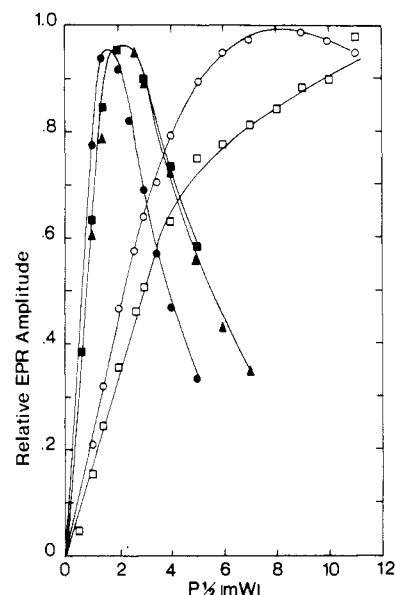


Figure 10. EPR saturation plots of $L\text{-}trans\text{-}[CD(I_3)_y]_x$ for y values (●) 0, (■) 5.5×10^{-6} , (▲) 3.2×10^{-5} , (○) 7.4×10^{-3} , and (□) 1.3×10^{-2} .

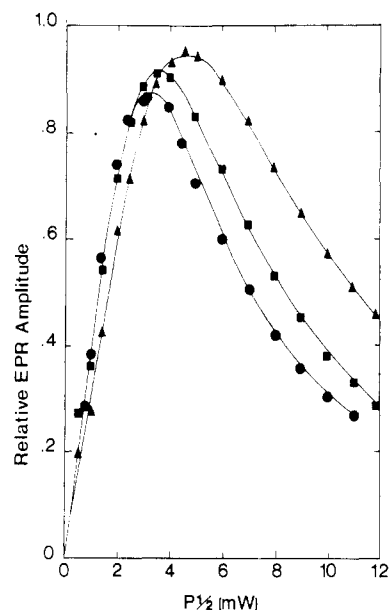


Figure 11. EPR saturation plots of $H\text{-}trans\text{-}[CH(I_3)_y]_x$ for y values (●) 0, (■) 4.5×10^{-4} , and (▲) 3.9×10^{-3} .

s for $0 \leq y \leq 8.3 \times 10^{-3}$. There was no detectable EPR at $y = 4.2 \times 10^{-2}$.

The very low and high MW $trans\text{-}[CH]_x$ and $trans\text{-}[CD]_x$ show quite similar variations of relaxation times with iodine doping as for $S\text{-}[CH]_x$.⁷ Doping decreases T_1 monotonically beginning at the ppm level of I_3^- , and T_2 remains relatively constant and decreases when $y > 3 \times 10^{-3}$. The only significant difference is that T_2 was unchanged by doping for the $\bar{M}_n = 870\,000$ sample.

Undoped and iodine-doped $L\text{-}trans\text{-}[CH]_x$ and $-[CD]_x$ have EPR characteristics that obey a Curie dependence. Figure 12 shows that their intensities increase about 1.8–1.9-fold with a 160 K decrease in temperature. These results are consistent with those obtained by Weinberger et al.¹⁵ for undoped $trans\text{-}[CH]_x$.

Discussion

Equilibrium Unpaired-Spin Concentration in Undoped $[CH]_x$. For optimum conditions of thermal isom-

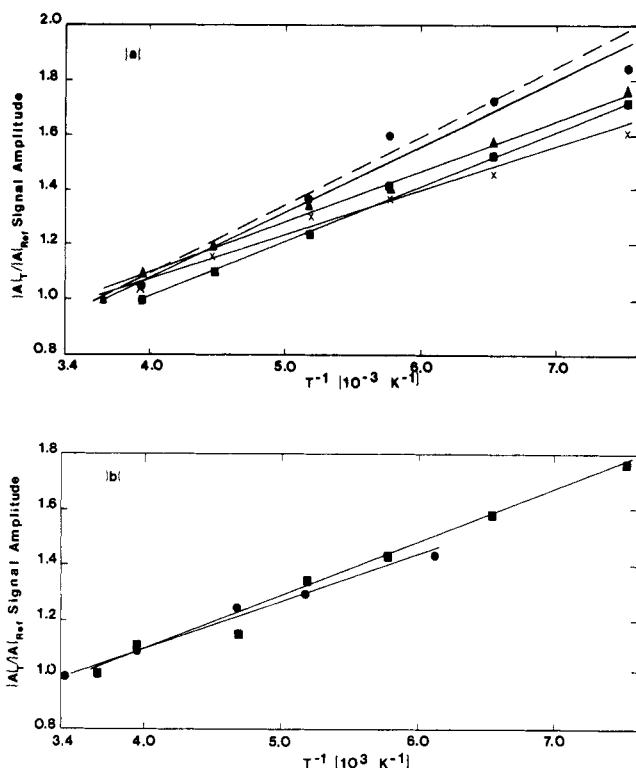
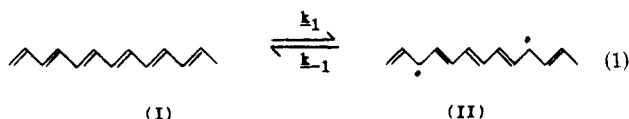


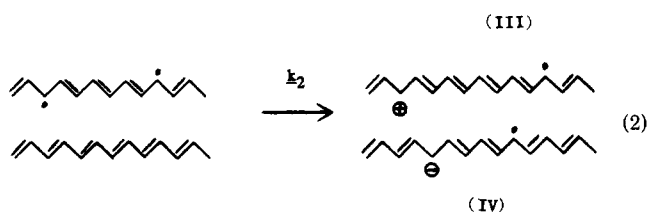
Figure 12. Temperature dependence of normalized integrated EPR intensity for (a) *L-trans*-[CH(I₃)_y]_x for *y* values (●) 0, (■) 4.6×10^{-6} , (▲) 3.5×10^{-4} , and (×) 1.3×10^{-3} and (b) *L-trans*-(CD(I₃)_y)_x for *y* values (●) 0, (■) 7.9×10^{-3} .

erization there is a relatively constant value of spin concentration of ca. 4.8×10^{-4} spin/CH for all the *trans*-[CH]_x polymers (Table II), as are most reported results of [S]_m in optimally isomerized *trans*-[CH]_x. In contrast, if this [S]_m is expressed as spin per chain, it has values of 0.02, 0.4, and 32 for [CH]_x with *M_n* of 480, 11 000, and 870 000, respectively. Therefore [S]_m is not a chain property but a bulk property. In other words, unpaired spins are created within a chain, but annihilation occurs both by intrachain and interchain processes. Unpaired spins are formed in pairs by thermal isomerization; in the soliton concept, the neutral defects are formed in soliton-antisoliton pairs. Let *K* be the equilibrium constant for eq 1. The observed

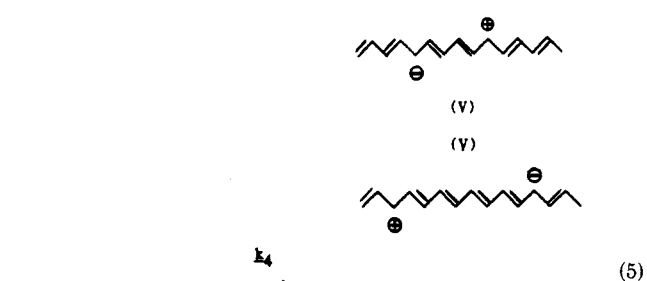
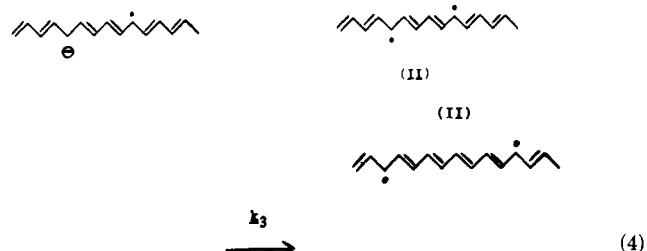
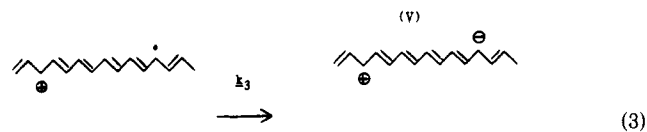


[S]_m cannot be the direct consequence of this equilibrium. The energy for the creation of a soliton-antisoliton pair is about 0.84 eV.⁴ At the typical isomerization temperature of 423 K, [S]_m would be only about 2×10^{-10} . Furthermore, if process 1 is truly reversible, [S] would decrease when the sample is returned to room temperature. This does not happen.

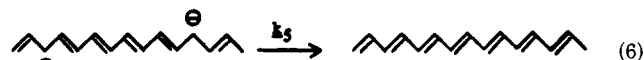
The fact that [S]_m is the same for *trans*-[CH]_x of all MW indicates the properties are controlled by interchain processes. A possible mechanism is the interchain hopping of an unpaired spin to a nearby chain, eq 2, whereby the



two unpaired spins became separated on different chains. The energy required is¹⁶ $E(p^+) + E(p^-) - 2E(S\cdot) \sim 1.3 - 0.84 = 0.46$ eV, where the energies are for the creation of a positive polaron, a negative polaron, and a neutral soliton, respectively. Interchain annihilation of unpaired spins in III and IV can result from intersoliton electron hopping processes¹⁷ (eq 3-5). Species II can undergo spin anni-



hilation with a rate constant k_{-1} . The positive and negative solitons can undergo exothermic neutralization with $k_5 \gg k_{-1}$.



Assuming pseudo stationary state for all the transient species, we have

$$[S\cdot]_m = \left(\frac{k_2 K}{k_4 + 2k_3} \right) [CH]_x \quad (7)$$

Therefore, [S]_m is only dependent on the concentration of CH units but independent of MW.

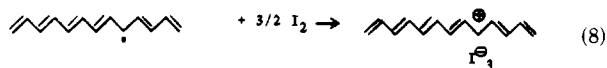
Spin Dynamics. In our previous study of *S-trans*-[CH]_x, we interpreted the decrease of *T*₁ by the ppm level of iodine doping^{5,7} as due to off-chain diffusion of spin, resulting in spin-orbit interaction between I₃⁻ and the spin. It was possible to obtain an estimate of *D*_⊥ from these data. The effect of iodine on *T*₂ occurs at much higher *y*(I₃⁻) $\sim 3 \times 10^{-4}$, from which we estimated a value on *D*_∥. In the case of *cis*-[CH]_x, the *T*₁ is not affected by small amounts of iodine dopant.

The present study shows that ppm of iodine doping also decreases *T*₁ of both *L-trans*-[CH]_x and *H-trans*-[CH]_x. Since independence of [S]_m on MW implies equally facile interchain spin diffusion, the effect of I₃⁻ on the reduction of *T*₁ should be the same for different MW *trans*-[CH]_x polymers. The value of *T*₂ for *L-trans*-[CH]_x is not affected by doping up to 1.3×10^{-3} . Between *y* = 1.3×10^{-3}

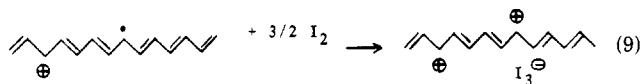
and 8.5×10^{-3} , T_2 started to decrease due to the spin-orbit interaction of the unpaired spin and I_3^- on the same chain. This behavior parallels that of *S-trans*-[CH]_x. In contrast, there is no reduction of T_2 in *H-trans*-[CH]_x up to $y(I_3^-) = 8.3 \times 10^{-3}$. It is possible that there is a barrier for in-chain spin diffusion in very high MW backbone. There are other possible complications, such as homogeneity of doping and dopant ion distribution along a long chain. The present results support the values of $D_{||}$ and D_{\perp} given earlier.⁵

In the case of *S-cis*-[CH]_x, iodine doping did not affect either T_1 or T_2 up to $y(I_3^-) = 1.3 \times 10^{-4}$. This is because the spins are immobile in the *cis* polymer and they cannot interact with small amounts of I_3^- . Above this dopant concentration the EPR cannot be saturated. In *L-cis*-[CH]_x, there is no influence of dopant on T_1 and T_2 even at $y(I_3^-) = 1.7 \times 10^{-3}$. This may be due to the fact that each dopant isomerizes a number of *cis* CH units that is greater than the 30 CH units in *L-cis*-[CH]_x. In the case in which there can be an effect of dopant on EPR relaxation times in high MW polymers, a spin after interchain hopping is more likely to encounter an I_3^- ion in a long chain. A short chain may not have a dopant ion at comparable $y(I_3^-)$.

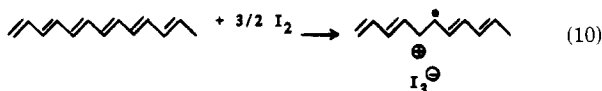
Effect of Doping on [S]_m. This study on high and low MW [CH]_x and the previous ones^{7,11} on $\bar{M}_n \sim 11000$ polymers leaves no doubt that chemical doping begins to decrease [S \cdot] when y exceeds 3×10^{-4} to 10^{-3} . This phenomenon had been observed by others as well¹⁸ but never explained. One might think that chemical doping would create almost as many S \cdot as it eliminates. For instance, if a chain already contains an S \cdot , the dopant can oxidize it directly, i.e.



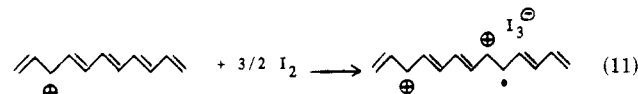
or



In contrast, direct oxidation of [CH]_x would create new S \cdot



or



Whether eq 8 and 9 or 10 and 11 are favored depends upon the [S \cdot]. In the case of *trans*-[CH]_x with [S \cdot]_m $\sim 4.8 \times 10^{-4}$, no detectable change in [S \cdot] for y less than this value would be expected. In the case of *cis*-[CH]_x with low initial value [S \cdot], doping increases its concentration because reactions 8 and 9 are of low probability.

To explain the disappearance of S \cdot commencing at $y \sim 3 \times 10^{-4}$, we note that the binding energy of polaron in species III and IV had been estimated to be 0.07–0.3 eV.^{16b,19} Reaction 5, which is the main process for interchain annihilation of S \cdot , is slow. We have pointed out^{11,20} that the charge carriers are in a glassy state with very low mobility at low dopant concentration. At $y \sim 3 \times 10^{-4}$ for homogeneously doped samples, there is a carrier mobility transition or carrier "glass" transition due to screening of Coulombic potential. As the carrier becomes free, there

is a concomitant reduction of polaron binding energy. This would result in a large increase in k_4 for reaction 5 and a decrease of [S \cdot] in eq 7. The fact that this decrease of [S \cdot] occurs at about the same dopant concentration for *cis*-[CH]_x as in *trans*-[CH]_x is consistent with doping-induced isomerization and the importance of interchain processes 2–5. This is further supported by the independence of MW for this phenomenon.

Conclusions

Before our MW determination for [CH]_x,⁸ there was no knowledge about this most fundamental property of this polymer. Together with the detailed kinetic study,⁹ it becomes possible to synthesize [CH]_x with a known \bar{M}_n . In fact, the radiotagging technique can determine the variation of \bar{M}_n over a large film of [CH]_x in a given preparation.^{8b} Characterizations of [CH]_x of very different MW showed that they exhibit similar properties,¹⁰ except that the *L-cis*-[CH]_x undergo thermal isomerization more readily and completely than the higher MW polymers.

Some EPR properties of undoped [CH]_x have MW dependencies as one would expect. Therefore, both *L-cis*- and *L-trans*-[CH]_x have longer T_1 than the corresponding higher MW polymers. This may be attributed to shorter correlation time for the low MW chains. However, most other EPR properties are insensitive to MW from 500 to 870000; these include (1) the maximum unpaired-spin concentrations in *trans*-[CH]_x; (2) T_1 in *trans*-[CH]_x is lowered by ppm of iodine doping and decreases monotonically with increasing y ; (3) T_2 in *trans*-[CH]_x is unaffected by doping until y exceeds 3×10^{-4} and then it decreases with increasing y ; (4) [S \cdot] in *trans*-[CH]_x is not changed by doping up to $y \sim 3 \times 10^{-4}$, above which [S \cdot] decreases abruptly; (5) [S \cdot] in *cis*-[CH]_x increases with doping up to $y \sim 3 \times 10^{-4}$ and then decreases as in *trans*-[CH]_x. All these properties are controlled by interchain diffusion or hopping of S \cdot , which are independent of MW.

Acknowledgment. This work was supported by a grant from the National Science Foundation.

Registry No. *cis*-Polyacetylene (homopolymer), 25768-70-1; *trans*-polyacetylene (homopolymer), 25768-71-2; iodine, 7553-56-2.

References and Notes

- (1) Ito, T.; Shirakawa, H.; Ikeda, S. *J. Polym. Sci., Polym. Chem. Ed.* **1974**, *12*, 11.
- (2) Ito, T.; Shirakawa, H.; Ikeda, S. *J. Polym. Sci., Polym. Chem. Ed.* **1975**, *13*, 1943.
- (3) Peierls, R. E. "Quantum Theory of Solids"; Clarendon Press: Oxford, 1955; p 108.
- (4) (a) Rice, M. *J. Phys. Lett. A* **1979**, *71*, 152. (b) Su, W. P.; Schrieffer, J. R.; Heeger, A. *J. Phys. Rev. B: Condens. Matter* **1980**, *22*, 2099; **1983**, *28*, 1138(E).
- (5) Chien, J. C. W. "Polyacetylene: Chemistry, Physics and Material Science"; Academic Press: New York, 1984.
- (6) (a) Goldberg, I. B.; Crowe, H. R.; Newman, P. R.; Heeger, A. J.; MacDiarmid, A. G. *J. Chem. Phys.* **1979**, *70*, 1132. (b) Weinberger, B. R.; Ehrenfreund, E.; Pron, A.; Heeger, A. J.; MacDiarmid, A. G. *J. Chem. Phys.* **1980**, *72*, 4749. (c) Chien, J. C. W.; Karasz, F. E.; Wnek, G. E. *Nature (London)* **1980**, *285*, 390.
- (7) Chien, J. C. W.; Wnek, G. E.; Karasz, F. E.; Warakowski, J. M.; Dickinson, L. C.; Heeger, A. J.; MacDiarmid, A. G. *Macromolecules* **1982**, *15*, 614.
- (8) (a) Chien, J. C. W.; Capistran, J. D.; Karasz, F. E.; Dickinson, L. C.; Schen, M. A. *J. Polym. Sci., Polym. Lett. Ed.* **1983**, *21*, 93. (b) Chien, J. C. W.; Karasz, F. E.; Schen, M. A.; Hirsch, J. A. *Macromolecules* **1983**, *16*, 1694.
- (9) Schen, M. A.; Karasz, F. E.; Chien, J. C. W. *J. Polym. Sci., Polym. Chem. Ed.* **1983**, *21*, 2787.
- (10) Chien, J. C. W.; Schen, M. A. *J. Polym. Sci., Polym. Chem. Ed.* **1985**, *23*, 2447.
- (11) Chien, J. C. W.; Warakowski, J. M.; Karasz, F. E.; Chia, W. L.; Lillya, C. P. *Phys. Rev. B: Condens. Matter* **1983**, *28*, 6937.

- (12) (a) Chien, J. C. W.; Karasz, F. E.; Wnek, G. E.; MacDiarmid, A. C.; Heeger, A. J. *J. Polym. Sci., Polym. Lett. Ed.* **1979**, *18*, 45. (b) Bernier, P.; Rolland, M.; Linays, C.; Disi, M. *Polymer* **1980**, *21*, 7.
- (13) Chien, J. C. W.; Yang, X. *J. Polym. Sci., Polym. Lett. Ed.* **1983**, *21*, 767.
- (14) Epstein, A. J.; Rommelmann, H.; Druy, M. A.; Heeger, A. J.; MacDiarmid, A. G. *Solid State Commun.* **1981**, *38*, 683.
- (15) Weinberger, B. R.; Kaufer, J.; Heeger, A. J.; Pron, A.; MacDiarmid, A. G. *Phys. Rev. B: Condens. Matter* **1979**, *20*, 223.
- (16) Campbell, D. K.; Bishop, A. R. *Phys. Rev. B: Condens. Matter* **1981**, *24*, 4859. (b) Bredas, J. L.; Chance, R. R.; Silbey, R. *Phys. Rev. B: Condens. Matter* **1982**, *26*, 5843 (1982).
- (17) (a) Kivelson, S. *Phys. Rev. Lett.* **1981**, *46*, 1344. (b) Kivelson, S. *Phys. Rev. B: Condens. Matter* **1982**, *25*, 3798.
- (18) (a) Ikehata, S.; Kaufer, J.; Woerner, T.; Pron, A.; Druy, M. A.; Sivak, A.; Heeger, A. J.; MacDiarmid, A. G. *Phys. Rev. Lett.* **1980**, *45*, 1123. (b) Epstein, A. J.; Rommelmann, H.; Druy, M. A.; Heeger, A. J.; MacDiarmid, A. G. *Solid State Commun.* **1981**, *38*, 683.
- (19) (a) Su, W. P.; Schrieffer, J. R. *Proc. Natl. Acad. Sci. U. S. A.* **1980**, *77*, 5626. (b) Bryant, G. W.; Glick, A. J. *Phys. Rev. B: Condens. Matter* **1982**, *26*, 5855.
- (20) Chien, J. C. W.; Babu, G. N. *J. Chem. Phys.* **1985**, *82*, 441.

Polarized Raman Measurements of Structural Anisotropy in Uniaxially Oriented Poly(vinylidene fluoride) (Form I)

Laurie Lauchlan and John F. Rabolt*

IBM Almaden Research Center, San Jose, California 95120. Received March 26, 1985

ABSTRACT: The anisotropic scattering properties of a uniaxially oriented filament of planar zigzag (form I) poly(vinylidene fluoride) have been investigated by polarized Raman scattering measurements. Results indicate that the assignment of the observed bands to specific symmetry species is straightforward and suggest that IR and Raman bands previously assigned from studies on drawn films should be reexamined. Comparison of these new assignments with those calculated from existing valence force fields gives a reasonable agreement but suggests that the force field could be improved by refinement incorporating these latest results. In addition, the observation of a low-frequency Raman active longitudinal acoustical mode and the correlation of its frequency with the crystalline stem length obtained from small-angle X-ray scattering and crystallinity measurements are shown to reflect the trans planar conformation of form I.

Introduction

Considerable interest in poly(vinylidene fluoride) (PVF₂) continues to exist because of the piezo- and pyroelectric properties that are exhibited by certain of its crystalline forms.¹⁻³ Recently it has also been shown that random copolymers of vinylidene fluoride and trifluoroethylene exhibit ferroelectric behavior over a specific range of comonomer concentration,⁴ again leading to a flourish of research activity^{5,6} designed to understand the mechanism responsible for this effect.

Although vibrational spectroscopy, in general, has played only a minor role in unraveling the physics of piezoelectricity in polymers, it has played a more important role in identifying the conformational structure of the molecular backbone responsible for piezoelectric behavior. Infrared studies⁷⁻¹¹ have been reported on all three crystalline forms of PVF₂ with band assignments being made from polarized measurements obtained from oriented films. In most cases agreement between the observed bands and those determined from normal coordinate calculations has been satisfactory,^{10,11} but a complete set of assignments has not been available.

On the other hand Raman studies¹² on oriented films have been much more complicated due to the relatively small thickness of films after orientation (hence a small scattering volume) and, perhaps more seriously, polarization scrambling of the incident and scattered light due to domains in the film that reduce its transparency in the visible. This latter problem is a general one in polymers and, as such, has prevented Raman polarization studies in all but the simplest cases. The potential of such studies is great since, together with a group theoretical analysis, it provides a means of identifying the symmetry of the observed bands, information that can then be used to refine existing force fields.^{10,11} Another important utility

of polarized Raman measurements is to differentiate between proposed conformational structures since, in many cases, alternate structures dictate a different set of spectroscopic selection rules from which a comparison with experimental observations can be made.

Our own studies¹³ of anisotropic Raman scattering in uniaxially oriented polymers have progressed over the past several years because of the availability of transparent highly oriented monofilaments that have found use in high-modulus applications. Recently, in Raman studies on an alternating copolymer of ethylene and tetrafluoroethylene (E-TFE)¹³ it was determined that the conformational structure was, in fact, planar zigzag, not helical, a subject of some controversy in the past.^{14,15} In order to draw that conclusion from polarized Raman measurements, a group theoretical formalism was derived¹⁶ to predict spectroscopic activity for polymers whose main axis of symmetry is perpendicular to the direction of uniaxial orientation. These expressions are generally applicable to all planar zigzag structures and thus have been applied to a study of PVF₂ (form I) in this current work. In conjunction with this analysis the anisotropic scattering properties of a highly oriented uniaxial filament were measured in a number of sample geometries, allowing specific band assignments to be made. A set of revised band assignments is proposed and reasons for discrepancies with previous work are discussed.

Experimental Section

The PVF₂ sample used in this study was provided as a 0.01-in. diameter filament by Albany Monofilament Co. It was produced by extrusion through a pinhole die followed by a ~4× draw. The source of the PVF₂ polymer was Pennwalt Corp., and, as such, this material contained 5-6% head-head defects.

Polarized Raman measurements were obtained with a Jobin-Yvon HG-2S double monochromator equipped with an RCA